#### Research Article

Yan-bo Chen, Yong Deng\*, Ran Liu, Li-da Chen, and Xing-min Guo

# Optimization of alkali metals discharge performance of blast furnace slag and its extreme value model

https://doi.org/10.1515/htmp-2022-0013 received October 17, 2021; accepted December 19, 2021

Abstract: In order to improve the alkali metals discharge capacity of slag, the gas-slag balance method was used to carry out the slag alkali metals discharge experiments, the effect of slag composition on alkali metals discharge performance of slag was studied, some suggestions were put forward to optimize the alkali metals discharge performance of slag and the extreme value model was established. The results show that the alkali metals discharge ratio of slag decreased with the increase in the binary basicity and mass fraction of TiO2, and increased with the increase in the mass fraction of MgO, Al<sub>2</sub>O<sub>3</sub> and MnO. The change in slag composition led to the change in the solubility of alkali metal oxides in liquid slag, decomposition of alkali metal silicates, structure of the slag in liquid state and viscosity of the slag, and then affected the alkali metals discharge performance of slag. The ability of slag to absorb alkali metals was certain under the condition of fixed composition. With the help of slag alkali metals discharge extreme value model, whether the current slag meets the needs of blast furnace alkali metals discharge could be evaluated. The alkali metals discharge capacity of slag could be improved by optimizing the alkali metals discharge performance of slag combined with experiments and actual production.

Yan-bo Chen, Xing-min Guo: School of Metallurgical and Ecological Engineering, University of Science and Technology Beijing, Beijing 100083. China

Ran Liu, Li-da Chen: Institute for Metallurgical Engineering and Technology, North China University of Science and Technology, Tangshan 063210, Hebei, China

**Keywords:** blast furnace, slag alkali metals discharge, influence mechanism, performance optimization, extreme value model

### 1 Introduction

Greening and intelligent are the inevitable requirements for the transformation and upgrading of iron and steel industry, which will promote the development of blast furnace (BF) in the direction of large scale and refinement [1–3]. The large scale and refinement BF puts forward higher standards for the quality of raw materials and fuels, especially for the control of harmful elements (alkali metals, lead, zinc, sulfur and arsenic) in raw materials and fuels, there is an upper limit of furnace load [4–8].

Alkali metals in raw materials and fuels not only worsens the low temperature reduction degradation property of sinter and pellet, but also affects the coke melting loss reaction and reduces the post reaction strength of coke, so the amount of powder in BF increases, the permeability of BF decreases and the differential pressure of BF increases [9–12]. There is a phenomenon of "cyclic enrichment" after alkali metals enter BF, it will form "nodules" on the hot surface of the furnace lining after enrichment to a certain extent, and change the operation furnace profile of BF [13]. Alkali metals steam can even enter the refractory of BF [14–19], making the refractory brittle and spalling, which seriously affects the service life of BF [20–25].

In this study, the optimization of slag alkali metals discharge based on experiments was carried out to improve the alkali metals discharge capacity of slag, and the extreme value model was established to evaluate the alkali metals discharge capacity of slag. The slag alkali metals discharge experiments were designed by using the gas-slag balance method to explore the influence law of basicity and composition content on alkali metals discharge ratio of slag, and clarify the effect of basicity and composition on alkali metals discharge performance of slag. The optimization

<sup>\*</sup> Corresponding author: Yong Deng, Institute for Metallurgical Engineering and Technology, North China University of Science and Technology, Tangshan 063210, Hebei, China, e-mail: ustbdy@126.com

scheme of alkali metals discharge performance of slag was proposed based on the analysis of the experimental results. The extreme value model of slag alkali metals discharge was established to calculate the current extreme value of BF slag alkali metals discharge.

### 2 Experimental

### 2.1 Samples preparation and experimental setup

The mass fraction of actual slag composition in an ironmaking plant was taken as the benchmark for slag alkali metals discharge experiments. It was prepared with CaO, MgO, Al<sub>2</sub>O<sub>3</sub>, SiO<sub>2</sub>, MnO and TiO<sub>2</sub> pure chemical reagent powder. Among them, alkali metals were mixed into slag in the form of K<sub>2</sub>CO<sub>3</sub> and Na<sub>2</sub>CO<sub>3</sub>. Q6 The slag sample was  $50 \,\mathrm{g}$ ,  $3.10 \,\mathrm{g}$  for  $\mathrm{K}_2\mathrm{CO}_3$  and  $5.40 \,\mathrm{g}$  for  $\mathrm{Na}_2\mathrm{CO}_3$ . The weighed sample powder was poured into a mortar for mixing, and the mixed powder was packed into a high-purity graphite crucible ( $\Phi$ 64 mm  $\times$  90 mm). The mass fraction of the experimental slag is shown in Table 1. The vertical tubular furnace was used for slag alkali metals discharge experiments, the inside of the tubular furnace was a corundum tube, U-shaped silicon molybdenum rod was employed as the heating unit and the insulation material is alumina refractory fiber, and the maximum temperature can reach 1.600°C.

#### 2.2 Experimental procedure

The gas-slag (alkali metals steam and slag) balance method was employed to carry out the slag alkali metals discharge experiments. The high-purity graphite crucible containing the mixed powder sample was put into the tubular furnace, the upper part of the graphite crucible was covered with a graphite cover, which could inhibit the discharge of K and Na steam at high temperature, so that the slag could fully contact and react with alkali metals. Then, the tubular furnace was covered, and high-purity argon gas was introduced into the furnace with a flow rate of 3 L·min<sup>-1</sup>. The FP93 temperature control meter started to heat up after the temperature rise program was set. When the temperature rose to 1,500°C (the actual slag iron temperature in hearth, the highest liquidus temperature in the samples is 1,442°C), the temperature was kept for 2h to make the slag composition uniform and fully react with alkali metals. After the

Table 1: The mass fraction of slag sample

Number	CaO	SiO <sub>2</sub>	MgO	Al <sub>2</sub> O <sub>3</sub>	MnO	TiO <sub>2</sub>	Basicity
A-1	36.62	39.38	8.50	15.50	0.00	0.00	0.93
A-2	37.81	38.19	8.50	15.50	0.00	0.00	0.99
A-3	38.93	37.07	8.50	15.50	0.00	0.00	1.05
A-4	39.98	36.02	8.50	15.50	0.00	0.00	1.11
A-5	40.98	35.02	8.50	15.50	0.00	0.00	1.17
A-6	41.92	34.08	8.50	15.50	0.00	0.00	1.23
B-1	40.51	36.49	7.50	15.50	0.00	0.00	1.11
B-3	39.45	35.55	9.50	15.50	0.00	0.00	1.11
B-4	38.93	35.07	10.50	15.50	0.00	0.00	1.11
B-5	38.40	34.60	11.50	15.50	0.00	0.00	1.11
C-1	40.51	36.49	8.50	14.50	0.00	0.00	1.11
C-2	40.24	36.26	8.50	15.00	0.00	0.00	1.11
C-4	39.72	35.78	8.50	16.00	0.00	0.00	1.11
C-5	39.45	35.55	8.50	16.50	0.00	0.00	1.11
D-1	39.88	35.92	8.50	15.50	0.20	0.00	1.11
D-2	39.77	35.83	8.50	15.50	0.40	0.00	1.11
D-3	39.67	35.73	8.50	15.50	0.60	0.00	1.11
D-4	39.56	35.64	8.50	15.50	0.80	0.00	1.11
D-5	39.45	35.55	8.50	15.50	1.00	0.00	1.11
E-1	39.45	35.55	8.50	15.50	0.00	1.00	1.11
E-2	38.93	35.07	8.50	15.50	0.00	2.00	1.11
E-3	38.40	34.60	8.50	15.50	0.00	3.00	1.11
E-4	37.88	34.12	8.50	15.50	0.00	4.00	1.11
E-5	37.35	33.65	8.50	15.50	0.00	5.00	1.11

Note: Bold values mainly represent the parameters changed in the experiment.

reaction, the graphite crucible was taken out with crucible pliers and put into water for quenching, to keep the alkali metals content of slag in equilibrium. Then, the cooled slag sample was ground into powder, the mass fractions of K<sub>2</sub>O and Na<sub>2</sub>O in each slag sample were detected through chemical analysis under different experimental conditions, the alkali metals discharge ratio of slag was calculated to determine the alkali metals discharge capacity of slag under different conditions.

### 3 Results

#### 3.1 Micro morphology of slag after reaction

After the reaction, the cooled slag sample was cut (as presented in Figure 1), the cross section of the sample was inlaid with resin into electron microscope samples and the micro morphology of the slag was analyzed by scanning electron microscope-energy dispersive spectrometer (SEM-EDS). As shown in Figure 2(a), holes of different sizes were found in the slag near the surface layer. According to the EDS results (Figure 2(b)), the



Figure 1: Macro morphology of slag after reaction.

mass fractions of K and Na were 3.66 and 5.34% in the hole and its surrounding area, respectively, which proved that the alkali metals once stayed in the hole. The hole presented a horn shape with large outer side and small inner side (Figure 2(c) and (d)), it was speculated that it might be caused by the separation of alkali metals steam from slag during high temperature experiment. Figure 3 shows the EDS results of the cross section of slag sample

after reaction, it was clear from the figure that during the high temperature experiment, K and Na had been distributed throughout the slag after the experiment. The alkali metals steam that could not be absorbed would float up on the surface of the liquid slag and separated from the slag. This proved that the alkali metals discharge experiment of gas-slag balance method can evaluate the alkali metals discharge capacity of slag.

### 3.2 Influence of various factors on alkali metals discharge ratio of slag

The morphology of the slag with different binary basicity after reaction is shown in Figure 4. It is clear from the figure that when binary basicity was 0.93, the color of the slag was yellow and the surface was uneven after reaction, which proved that the slag had absorbed a large amount of the alkali metals. The sample with higher binary basicity had darker color and less alkali metals absorption. In addition, when binary basicity was 1.23, the slag had insufficient strength after cooling and was

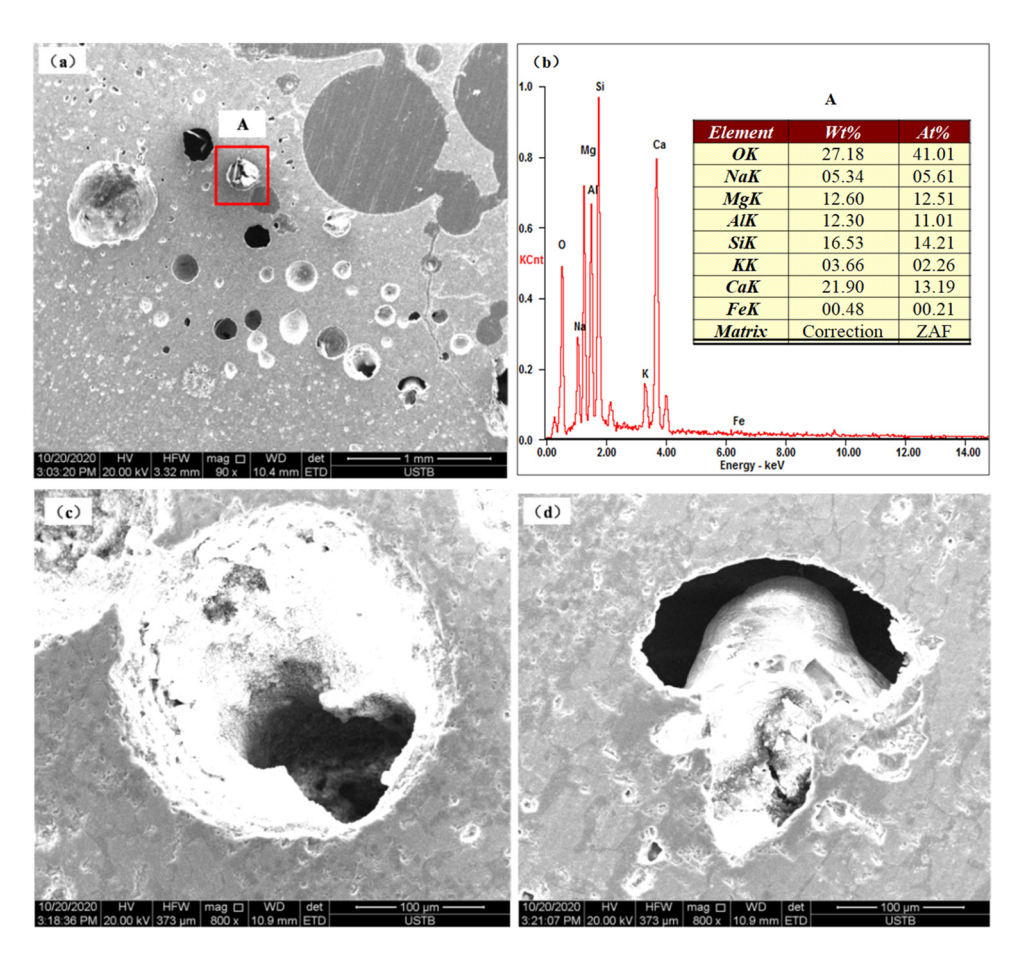


Figure 2: Micro morphology of slag after reaction. (a) Holes of different sizes; (b) EDS results of point A; (c) horn shaped hole; (d) internal morphology of the hole.

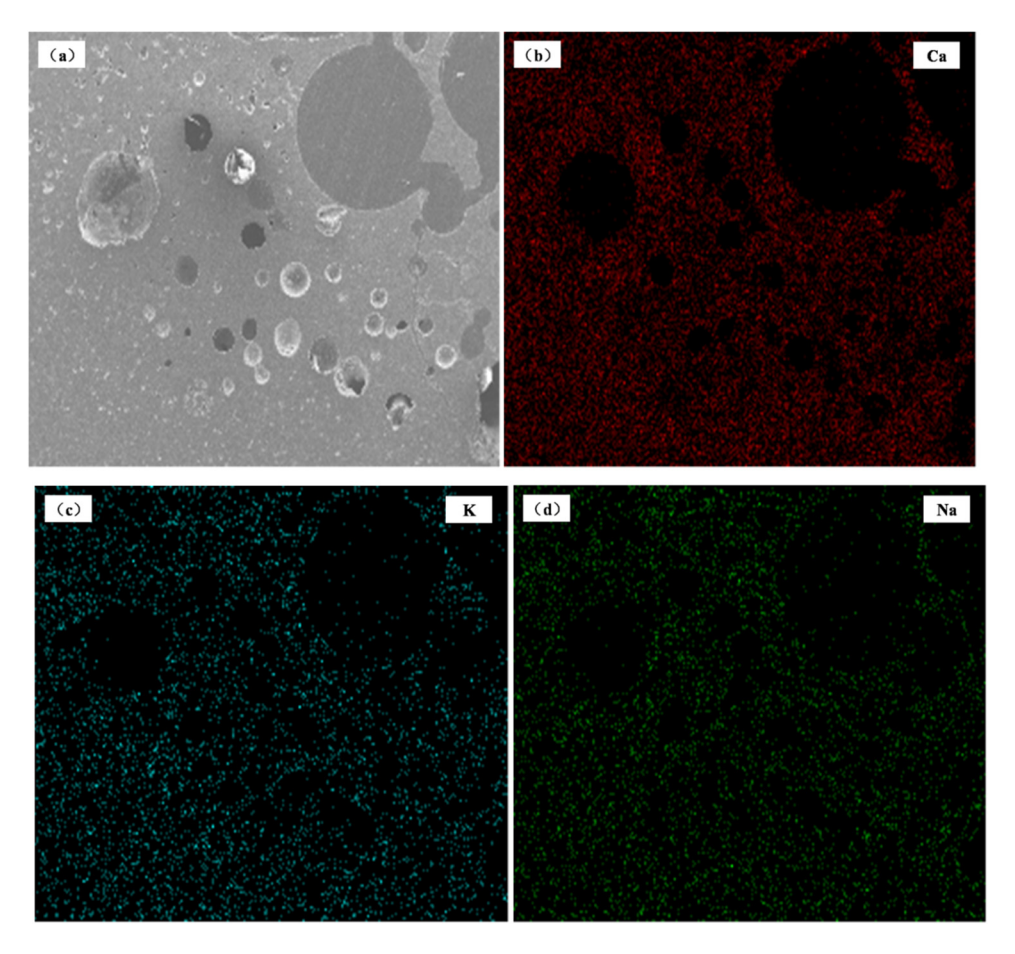


Figure 3: EDS results of the cross section of slag sample after reaction. (a) Morphology of slag cross section; (b) EDS result of Ca; (c) EDS result of K; (d) EDS result of Na..

broken into small pieces. It shows that the slag might not be able to absorb so much of alkali steam at this time, and the alkali metals steam overflowed from the slag during the experiment, resulting in a large number of holes left in the slag after cooling, enabling the slag sample to break easily.

The alkali metals discharge ratio of slag can be calculated as follows:

$$r = \frac{w_{(K_2O + Na_2O)} \times m_{\text{slag}}}{m_a},$$
 (1)

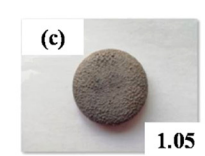
where r is the alkali metals discharge ratio of slag, %;  $w_{(K_2O+Na_2O)}$  is the total content of alkali metals in the slag after the experiment, %;  $m_{\rm slag}$  is the total mass of the

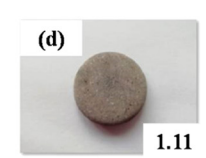
experimental slag, g; and  $m_a$  is the total mass of the alkali metals added in the experiment, g.

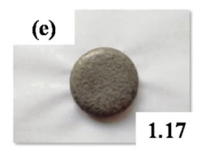
The influence of binary basicity on slag alkali metals discharge is shown in Figure 5. When the binary basicity of slag increased from 0.93 to 1.23, the alkali metals discharge ratio of slag decreased from 85.03 to 68.16%. The alkali metals discharge ratio of slag generally showed a downward trend. The mass fraction of alkali metals in the slag decreased with the increase in the binary basicity, that is, the alkali metals discharge capacity of the slag decreased with the increase in the binary basicity. When the binary basicity increased from 0.99 to 1.11, the alkali metals discharge ratio of the slag decreased from 85.03 to 73.04%, the degree of decline was obvious. However,











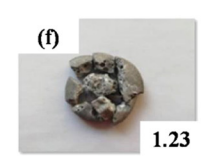


Figure 4: Morphology of slag with different binary basicity after reaction. (a) R = 0.93; (b) R = 0.99; (c) R = 1.05; (d) R = 1.11; (e) R = 1.17; (f) R = 1.23.

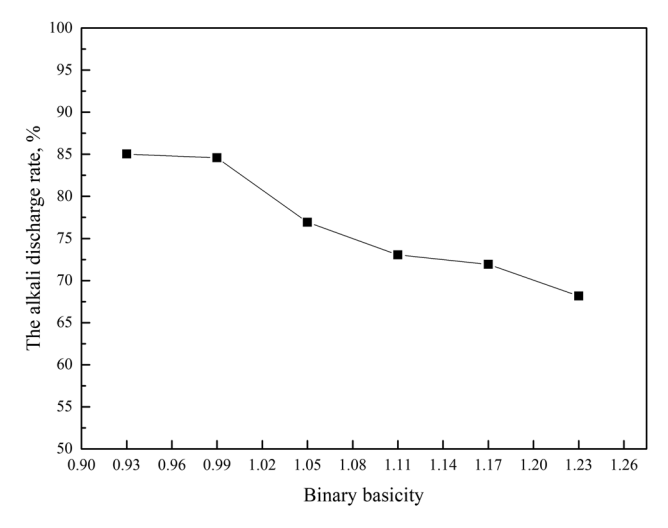


Figure 5: Effect of binary basicity on slag alkali metals discharge.

95 90 90 80 14.5 15.0 15.5 16.0 16.5 16.5

100

Figure 7: Effect of Al<sub>2</sub>O<sub>3</sub> on slag alkali metals discharge.

when the binary basicity was 1.17, the decrease in the slag alkali metals discharge ratio was small.

As shown in Figure 6, when the mass fraction of MgO increased from 7.5 to 11.5%, the alkali metals discharge ratio of the slag increased from 65.05 to 76.59%. It showed an upward trend, the alkali metals discharge capacity of the slag increased with the increase in the MgO mass fraction in the slag.

Figure 7 depicts the effect of  $Al_2O_3$  on the slag alkali metals discharge. When  $Al_2O_3$  in the slag increased from 14.5 to 16.5%, the alkali metals discharge ratio of the slag increased from 62.72 to 73.15%. The mass fraction of alkali metals in the slag increased with the increase in  $Al_2O_3$  mass fraction in the slag, the increase in  $Al_2O_3$  could improve the alkali metals discharge capacity of the slag.

It can be seen from Figure 8 that with the increase in MnO mass fraction in the slag, the alkali metals discharge ratio of the slag showed a slow upward trend. When the mass fraction of MnO increased from 0.2 to 0.6%, the alkali metals discharge ratio of slag increased from 73.26 to 73.60%, the alkali metals discharge capacity of the slag changed a little. When the mass fraction of MnO increased from 0.6 to 1.0%, the alkali metals discharge ratio of the slag increased from 73.60 to 77.48%, the alkali metals discharge capacity of the slag increased slowly.

As shown in Figure 9, the alkali metals discharge ratio of the slag showed a downward trend with the increase in  $\text{TiO}_2$  mass fraction in the slag, the alkali metals discharge capacity of the BF slag decreased with the increase in  $\text{TiO}_2$  mass fraction in the slag. However, the degree of decline was different in different  $\text{TiO}_2$  mass

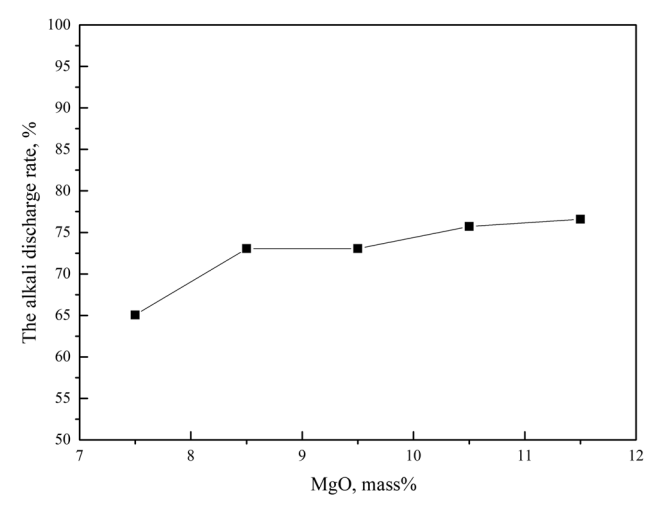


Figure 6: Effect of MgO on slag alkali metals discharge.

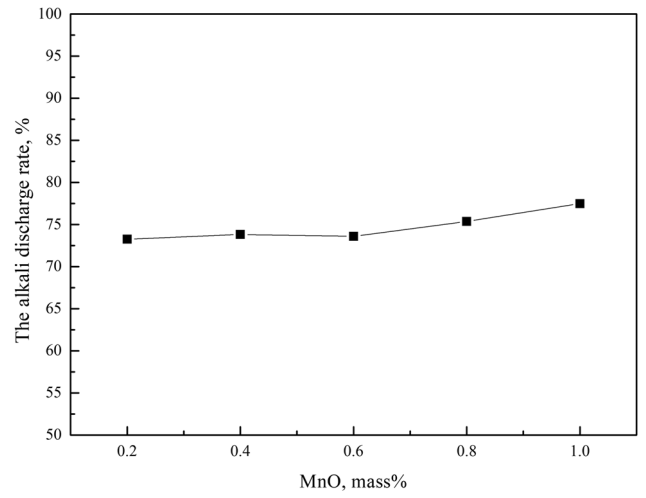


Figure 8: Effect of MnO on slag alkali metals discharge.

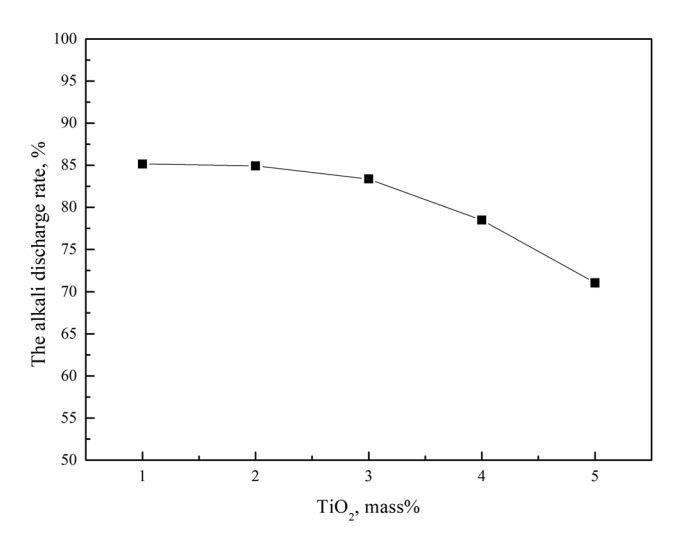


Figure 9: Effect of TiO<sub>2</sub> on slag alkali metals discharge.

fraction ranges. When the mass fraction of  $TiO_2$  was less than 3.0%, the alkali metals discharge ratio decreased from 85.14 to 83.37%, the decline was small. While, when the mass fraction of  $TiO_2$  was greater than 3.0%, the alkali metals discharge ratio decreased from 83.37 to 71.04%, the decline was large.

### 4 Discussion

## 4.1 Influence mechanism of slag composition on alkali metals discharge performance

Binary basicity. The alkali metals discharge capacity of the slag decreased with the increase in binary basicity. The mechanism: (1) The solubility of alkali metal oxides in the liquid slag decreased with the increase in binary basicity, so the alkali metals absorption capacity of the slag decreased after the increase in binary basicity. (2) Alkali metals were dissolved in the liquid slag and existed in the form of silicate, the following reactions occurred [26]:  $K_2SiO_3 + CaO + C = CaO \cdot SiO_2 + CO(g) + 2 K(g)$ . The mass fraction of CaO in the slag also increased with the increase in binary basicity, which would promote the reaction to the right, accelerate the decomposition of alkali metals silicate and reduce the alkali metals absorption capacity of the slag. When the binary basicity was 1.17, the decrease in the slag alkali metals discharge ratio was small, which might be related to the change in slag viscosity. In a certain range, the complex anion groups in

the slag were disintegrated into simple ion units to reduce the viscosity after the binary basicity increased. The kinetics of alkali metals discharge chemical reaction were improved, this was conducive to the alkali metals discharge reaction, and some adverse effects on alkali metals discharge were offset. However, when the binary basicity was too high (1.23), heterogeneous high melting point compounds such as  $2\text{CaO}\cdot\text{SiO}_2$  were formed in the slag, which increased the viscosity and further worsened the alkali metals discharge capacity of the slag. Therefore, excessive slag viscosity was unfavorable to alkali metals discharge.

*MgO*. The alkali metals discharge capacity of the slag increased with the increase in MgO mass fraction in the slag. The mechanism: (1) MgO could improve the solubility of alkali metals oxides in the liquid slag [27]. (2) The existence of MgO increased the free oxygen ion O<sup>2-</sup> in the liquid slag, the complex network ion structure and heterogeneous high melting point compounds in the slag were disintegrated. The structure of slag in the liquid state was simplified, so the viscosity of the slag was reduced. The components had greater diffusion kinetic energy in the liquid slag after the slag viscosity reduced, the kinetics of alkali metals discharge chemical reaction was improved, so the alkali metals discharge capacity of the slag was increased.

 $Al_2O_3$ . The increase in  $Al_2O_3$  mass fraction could improve the alkali metals discharge capacity of the slag. The mechanism: (1)  $Al_2O_3$  could form nepheline with high melting point (such as KAlSiO<sub>4</sub>) with SiO<sub>2</sub> and alkali metals in the slag, so that part of the alkali metals could be solidified in the slag [28,29]. (2)  $Al_2O_3$  could form CaO·Al<sub>2</sub>O<sub>3</sub> with CaO, reducing the mass fraction of free CaO and inhibiting the decomposition of alkali metal silicates, which made more alkali metals stay in the slag, so as to increase the alkali metals discharge capacity of the slag.

*MnO*. The alkali metals discharge ratio of the slag increased slowly with the increase in MnO mass fraction in the slag. The mechanism was mainly because MnO reduced the viscosity of the slag: (1) MnO could separate the free oxygen ion O<sup>2-</sup> from the slag, the free oxygen ion dissociated the complex network structure of the slag into a simple structure and reduced the viscosity of the slag. (2) MnO and SiO<sub>2</sub> formed manganese olivine (2MnO·SiO<sub>2</sub>) with low melting point in the slag, the superheat degree of the slag was increased, the force between the components in the liquid slag was reduced, so the viscosity of the slag was reduced. (3) The reduction of some oxides in the slag would release some CO gas, and the alkali metals steam would overflow from the slag with CO. When the mass fraction of MnO was high

(higher than 0.06%), it could inhibit the reduction of some oxides:  $2MnO + Ti = 2Mn + TiO_2$ , the foaming probability in the liquid slag was reduced [30,31]. The overflow of some alkali metals steam was restrained, so the alkali metals discharge capacity of the slag was improved.

 $TiO_2$ . The alkali metals discharge ratio of the slag showed a downward trend with the increase in TiO2 content in the slag. The mechanism: (1) The acidity of TiO<sub>2</sub> in the slag was weaker than that of SiO<sub>2</sub>, which was only about three fifths of that of SiO2. When the mass fraction of TiO<sub>2</sub> increased, the acidity of the slag was reduced, so the alkali metals discharge capacity was relatively reduced. (2) Some alkali metals could be dissolved by high melting point compound (perovskite) and low melting point compound (diopside) formed by TiO<sub>2</sub> in the slag. However, TiO<sub>2</sub> could precipitate solid particles such as TiC in the slag under high temperature and carbon containing conditions [32]. Once solid particles appeared in the liquid slag, the properties of Newtonian fluid would be changed and the viscosity of the slag would increase rapidly, so the kinetic conditions of alkali metals discharge chemical reaction were deteriorated. this effect completely masked the solid solution. In particular, when the mass fraction of TiO2 was high (higher than 3%), the viscosity increased greatly, so the alkali metals discharge capacity of the slag decreased significantly.

### 4.2 Optimization of slag alkali metals discharge performance

The alkali metals discharge performance of the slag was optimized based on the experimental results and theoretical analysis.

The alkali metals discharge capacity of the slag decreased with the increase in binary basicity under the condition of experimental slag system, the alkali metals discharge ratio of slag decreased little when the binary basicity was 1.17. Therefore, in the actual production process, on the premise of ensuring the production of qualified pig iron, it is suggested that the binary basicity should be controlled at about 1.17, considering desulfurization, alkali metals discharge and viscosity.

The alkali metals discharge capacity of the slag increased with the increase in MgO mass fraction in the slag. The mass fraction of MgO in the slag should not exceed 12%, in order to ensure the smooth operation of the BF, prevent the formation of high melting point periclase and spinel in the slag, deteriorate the fluidity of the slag and worsen the dynamic conditions of the reaction in the furnace. The mass fraction of

MgO in the BF slag is recommended to be controlled at 7.5–10.5% according to the actual slag system.

The alkali metals discharge ratio of the slag increased with the increase in  $Al_2O_3$  mass fraction in the slag; however, the slag viscosity increased with the increase in  $Al_2O_3$  mass fraction. Therefore, it is suggested that in the actual production process of BF, slag desulfurization, slag alkali metals discharge and slag viscosity should be comprehensively considered, and the mass fraction of  $Al_2O_3$  should be kept below 16%.

The alkali metals discharge ratio of the slag could be improved by increasing the mass fraction of MnO in the slag. However, the fluidity of the slag would increase with the high MnO content in it, which was unfavorable to the long service life of the hearth. Therefore, it is suggested that the mass fraction of MnO in slag should be controlled below 0.6%.

The alkali metals discharge capacity of the slag decreased with the increase in  ${\rm TiO_2}$  content in the slag. When the mass fraction of  ${\rm TiO_2}$  in the slag was high, solid particles such as TiC were precipitated in the slag, which made the viscosity of the slag increase rapidly. Therefore, it is recommended to reduce the mass fraction of  ${\rm TiO_2}$  in the slag as much as possible, during normal production of BF. Subsequently, the mass fraction of  ${\rm TiO_2}$  in the slag shall be appropriately increased according to the need of corrosion resistance and hearth protection.

### 4.3 Extreme value model of slag alkali metals discharge

BF slag itself has the ability to discharge alkali metals, but under the condition of fixed composition, the ability of the slag system to absorb alkali metals is limited. If the alkali metals load in the furnace exceeds the alkali metals discharge capacity of the slag system, the alkali metals will be "recycled and enriched" in the BF, which will have a series of adverse effects on the BF. Therefore, it is necessary to study the extreme value model of slag alkali metals discharge. The model is used to calculate the current extreme value of BF slag alkali metals discharge, evaluate the current situation of BF alkali metals discharge and judge whether the current slag can meet the needs of BF alkali metals discharge.

First, the mass fractions of  $K_2O$  and  $Na_2O$  in the slag are detected under the condition of existing slag composition. Take the highest value of the sum of different alkali metals' mass fractions:

$$w_{\text{max}} = w(K_2O) + w(Na_2O),$$
 (2)

where  $w_{\text{max}}$  is the highest value of total mass fraction of the slag alkali metals, %; and w(j) is the mass fraction of components in the slag, %.

The extreme value of alkali metals discharged with the slag is calculated under the condition of existing slag composition:

$$m_{\text{max}} = w_{\text{max}} \times R,$$
 (3)

where  $m_{\text{max}}$  is the extreme value of alkali metals discharged with the slag, kg·t<sup>-1</sup>; and R is the slag ratio of the BF, kg·t<sup>-1</sup>.

The alkali metals load of the BF is calculated according to the existing raw material conditions:

$$L = \sum_{i} [m_{i} \times w_{i}(K_{2}O) + m_{i} \times w_{i}(Na_{2}O)],$$
 (4)

where L is the alkali metals load of the BF, kg·tHM<sup>-1</sup>;  $m_i$  is the mass of different kinds of raw materials and fuels in the BF, kg·tHM<sup>-1</sup>; and  $w_i(j)$  is the alkali metals content in different kinds of raw materials and fuels, %.

The alkali metals load of the BF is compared with the extreme value of the slag alkali metals discharge, if  $L < m_{\rm max}$ , the BF slag can meet the needs of the alkali metals discharge; if  $L > m_{\rm max}$ , the BF slag under the existing conditions cannot complete the alkali metals discharge task, and it will produce "cyclic enrichment" in the BF. The existing slag composition needs to be adjusted to meet the needs of alkali metals discharge. The slag composition can be adjusted in the laboratory according to the slag alkali metals discharge performance optimization scheme. The mass fraction of alkali metals

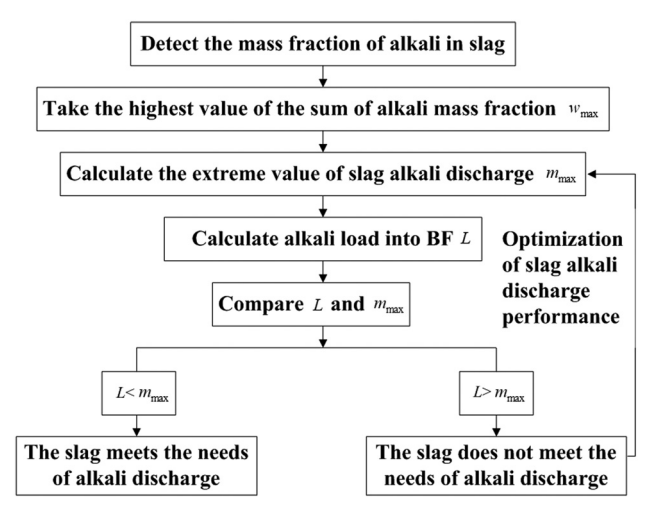


Figure 10: Technical route for adjusting slag alkali metals discharge performance.

in the slag is determined by the gas-slag balance experimental method in this article, and the extreme value of alkali metals discharge is calculated. If the experimental slag can meet the needs of alkali metals discharge, it can be put into practice in BF production. If the experimental slag still does not meet the alkali metals discharge needs, continue to adjust until it can meet the alkali metals discharge needs of the BF. The adjusted technical route is presented in Figure 10.

### 5 Conclusion

- (1) The influence direction and range of various factors on the alkali metals discharge ratio of the slag were different. The alkali metals discharge ratio of the slag decreased with the increase in binary basicity and mass fraction of TiO<sub>2</sub>. The alkali metals discharge ratio of the slag showed an upward trend with the increase in mass fraction of MgO, Al<sub>2</sub>O<sub>3</sub> and MnO.
- (2) The influence mechanism of slag composition on alkali metals discharge ratio: the alkali metals discharge performance of the slag was mainly affected by the solubility of alkali metal oxides in the liquid slag, the decomposition of alkali metal silicates, structure of slag in the liquid state and the viscosity of the slag.
- (3) In actual production, the ability of the slag system to absorb alkali metals was limited when the composition was fixed. With the help of the extreme value model of the slag alkali metals discharge, whether the current slag can meet the needs of the BF alkali metals discharge could be evaluated. The alkali metals discharge capacity of the slag could be improved by optimizing the alkali metals discharge performance of the slag combined with experiments and actual production.

**Funding information:** The project was supported by Open Fund of The State Key Laboratory of Refractories and Metallurgy (G202005), Natural Science Foundation–Steel and Iron Foundation of Hebei Province (E2020209069, E2020209208).

**Author contributions:** Yong Deng contributed to the conception of the study; Yan-bo Chen, Li-da Chen performed the experiment; Ran Liu, Xing-min Guo helped perform the analysis with constructive discussions.

Conflict of interest: Authors state no conflict of interest.

### References

- [1] Li, X. C. Road map to high-quality development of iron and steel industry in new age. Iron and Steel, Vol. 54, No. 1, 2019, pp. 1-7.
- Xiao, P. Innovation practice and future prospects of blast fur-[2] nace ironmaking technology. Iron and Steel, Vol. 56, No. 6, 2021, pp. 10-14, 34.
- [3] Yang, T. J., J. L. Zhang, Z. J. Liu, and K. J. Li. Development of ironmaking industry at the new situation. Ironmaking, Vol. 39, No. 5, 2010, pp. 1-9.
- [4] Zhang, S. Z., D. H. Gao, P. F. Wang, and G. P. Luo. Balance and control of potassium and sodium in No. 6 blast furnace of Baotou steel. China Metallurgy, Vol. 29, No. 3, 2019, pp. 28-31.
- Liu, W. W., Y. H. Qi, K. X. Jiao, and H. K. Li. Balance and control of alkali metal in No.6 blast furnace of Tisco. China Metallurgy, Vol. 30, No. 12, 2020, pp. 72-76.
- [6] Zheng, P. C., J. L. Zhang, Z. J. Liu, and Y. B. Chen. Effect of alkali metals on thermal properties of coke. China Metallurgy, Vol. 27, No. 5, 2017, pp. 19-28.
- [7] Gan, M. Y. and Z. H. Tang. Control practice of harmful elements in blast furnace of Liugang. Ironmaking, Vol. 39, No. 4, 2020, pp. 35-38.
- [8] Si, J. C. and H. Y. Wei. Control practice of harmful elements in blast furnace of Liugang. Ironmaking, Vol. 35, No. 1, 2016, pp. 54-57.
- [9] Jiao, K. X., J. L. Zhang, Z. J. Liu, C. L. Chen, and Y. X. Liu. Analysis of blast furnace hearth sidewall erosion and protective layer formation. ISIJ International, Vol. 56, No. 11, 2016, nn. 1956-1963.
- [10] Dastidar, M. G., A. Bhattacharyya, B. K. Sarkar, D. Rajib, M. K. Mitra, and J. Schenk. The effect of alkali on the reaction kinetics and strength of blast furnace coke. Fuel, Vol. 268, 2020, id. 117388.
- [11] Wang, G. Influence of alkali metals on metallurgical properties of raw materials in blast furnace. Shanxi Metallurgy, Vol. 41, No. 5, 2018, pp. 17-19.
- [12] Xu, L. Effect of alkali metals on metallurgical properties of blast furnace raw materials. China Steel Focus, Vol. No. 15, 2019, pp. 15-16.
- [13] Xia, Z. H., Y. Sun, L. Chen, and J. W. Ge. Lump detection of No. 2 blast furnace in Shagang and recovery of furnace condition. Ironmaking, Vol. 36, No. 3, 2017, pp. 47-48.
- [14] Wang, T. S., Y. W. Li, S. B. Sang, Y. B. Xu, and H. Wang. Effect of pitch powder addition on the microstructure and properties of carbon blocks for blast furnace. Ceramics International, Vol. 45, No. 1, 2019, pp. 634-643.
- [15] Dai, Y. J., Y. C. Yin, X. F. Xu, S. L. Jin, Y. W. Li, and H. Harmuth. Effect of the phase transformation on fracture behaviour of fused silica refractories. Journal of the European Ceramic Society, Vol. 38, No. 16, 2018, pp. 5601-5609.
- [16] Dai, Y. J., Y. W. Li, X. F. Xu, Q. Y. Zhu, W. Yan, S. L. Jin, et al. Fracture behaviour of magnesia refractory materials in tension with the Brazilian test. Journal of the European Ceramic Society, Vol. 39, No. 16, 2019, pp. 5433-5441.
- [17] Dai, Y. J., Y. W. Li, S. L. Jin, H. Harmuth, Y. Wen, and X. F. Xu. Mechanical and fracture investigation of magnesia refractories with acoustic emission-based method. Journal of the European Ceramic Society, Vol. 40, No. 1, 2020, pp. 181-191.

- [18] Cheng, Y., T. B. Zhu, Y. W. Li, S. B. Sang, N. Liao, Z. P. Xie, et al. Microstructure and mechanical properties of oscillatory pressure sintered WC ceramics with different carbon sources. Ceramics International, Vol. 47, No. 8, 2021, pp. 11793-11798.
- [19] Chen, Q. L., T. B. Zhu, Y. W. Li, Y. Chen, N. Liao, L. P. Pan, et al. Enhanced performance of low-carbon MgO-C refractories with nano-sized ZrO<sub>2</sub>-Al<sub>2</sub>O<sub>3</sub> composite powder. Ceramics International, Vol. 47, No. 14, 2021, pp. 20178-20186.
- [20] Peng, W. D., Z. Chen, W. Yan, S. Schafföner, G. Q. Li, Y. W. Li, et al. Advanced lightweight periclase-magnesium aluminate spinel refractories with high mechanical properties and high corrosion resistance. Construction and Building Materials, Vol. 291, No. 11, 2021, id. 123388.
- [21] Xu, X. F., Y. W. Li, Y. J. Dai, T. B. Zhu, L. P. Pan, and J. Szczerba. Influence of graphite content on fracture behavior of MgO-C refractories based on wedge splitting test with digital image correlation method and acoustic emission. Ceramics International, Vol. 47, No. 9, 2021, pp. 12742-12752.
- [22] Liu, G. F., N. Liao, M. Nath, Y. W. Li, and S. B. Sang. Optimized mechanical properties and oxidation resistance of low carbon Al<sub>2</sub>O<sub>3</sub>-C refractories through Ti<sub>3</sub>AlC<sub>2</sub> addition. Journal of the European Ceramic Society, Vol. 41, No. 4, 2021, pp. 2948-2957.
- [23] Chang, Q. M., X. W. Li, H. W. Ni, W. Y. Zhu, C. G. Pan, and S. D. Hu. Modeling on dry centrifugal granulation process of molten blast furnace slag. ISIJ International, Vol. 55, No. 7, 2015, pp. 1361-1366.
- [24] Wang, Q. H., G. He, S. X. Deng, J. Liu, X. Y. Li, J. Q. Li, et al. Wetting behavior and reaction mechanism of molten Si in contact with silica substrate. Ceramics International, Vol. 45, No. 17, 2019, pp. 21365-21372.
- [25] Wang, T. S., S. B. Sang, and Y. W. Li. Effect of artificial graphite and nickel nitrate on the microstructure and properties of carbon blocks for blast furnace. Key Engineering Materials, Vol. 768, No. 4, 2018, pp. 267-273.
- [26] Lyu, Q., F. M. Li, L. N. Gu, and D. H. Hou. Experimental Investigation on dealkalization and desulphurization of Alkaliferous BF slag. Journal of Northeastern University, Vol. 28, No. 11, 2007, pp. 1590-1593.
- [27] Wang, Y. C., S. R. Na, C. Y. Chen, and R. J. Wang. Experimental Investigation on improving the capacity of removing Alkali metals of baogang blast furnace slag. Journal of Inner Mongolia University of Science and Technology, Vol. 20, No. 2, 2001, pp. 104-106, 117.
- [28] Peng, Q. C., B. Q. Chen, J. Peng, and L. M. Zhao. Discussion on alkali discharge of high Al<sub>2</sub>O<sub>3</sub> BF slag in Xiangtan iron & steel corp. Research on Iron & Steel, Vol. 34, No. 3, 2006, pp. 10-14.
- [29] Zhu, G. Y., J. L. Zhang, R. Mao, and X. Yuan. Orthogonal experimental study on removal of Alkalis through blast furnace slag. Research on Iron & Steel, Vol. 41, No. 6, 2013, pp. 19-23.
- [30] Qv, Y. P. and H. G. Du. Effect of MnO on foaming behavior of high titanium blast furnace slag. Journal of Northeastern University, Vol. 23, No. 8, 2002, pp. 769-772.
- [31] Li, Y. H., T. P. Lou, and Z. T. Sui. Effects of CaO and MnO on the crystallization of the Perovskite phase in the Ti-bearing blast furnace slag. Journal of Iron and Steel Research, Vol. 12, No. 3, 2000, pp. 1-4.
- [32] Chen, G. Y., J. L. Kang, S. J. Wu, L. X. Liu, F. Zhang, J. Peng, et al. Effect of TiO<sub>2</sub> on slag viscosity. Journal of Inner Mongolia University of Science and Technology, Vol. 37, No. 4, 2018, pp. 338-342, 372.